Validation of marine geoid models in the North Aegean Sea using satellite altimetry, marine GPS data and astrogeodetic measurements

Müller, A., Bürki, B., Limpach, P., Kahle, H.-G. (Geodesy and Geodynamics Laboratory, ETH Zurich, Switzerland)

Grigoriadis, V. N., Vergos, G. S., Tziavos, I. N., (Department of Geodesy and Surveying, Aristotle University of Thessaloniki, Greece)

Abstract. A dedicated measuring campaign for geoid determination has been carried out in the North Aegean Sea, Greece, in May 2005. It was realized in the frame of a joint project between the Geodesy and Geodynamics Laboratory (GGL) of ETH Zurich, and the Department of Geodesy and Surveying of the Aristotle University of Thessaloniki. The measurement area is part of the North Aegean Trough (NAT), which forms a continuation of the seismically active North Anatolian Fault Zone. Different methods for geoid determination have been applied, including astro-geodetic observations with the new Zenith Camera DIADEM in order to determine highly-precise Deflections of the Vertical (DoV), as well as GPS boat and buoy measurements to provide Sea Surface Heights (SSH). The data gathered during the campaign were compared to existing local gravimetric and altimetric geoid models. They helped to detect long wavelength errors in the gravimetric geoid model, which are mainly due to existing data gaps in the marine area.

Keywords. Geoid determination, North Aegean Trough, Zenith Camera DIADEM, Deflections of the Vertical, Marine GPS, Sea Surface Heights

1 Introduction

From the early seventies on, systematic attempts for precise geoid determination have been carried out in the Hellenic area. The recent gravimetric geoid solution HGFFT98 for the Hellenic area has been presented by Tziavos and Andritsanos (1999). In order to provide additional and independent data sets for an improved local geoid solution, a dedicated campaign was carried out in May 2005. The area under study is situated within $38° < \varphi < 42°$ N. and $22° < \lambda < 27°$ E. The measurement area forms part of the North Aegean Trough (NAT), which is considered to be a continuation of the seismically active North Anatolian Fault Zone. Highly-precise Deflections of the Vertical (DoV) have been observed with the digital Zenith Camera DIADEM, developed at GGL. Additionally, offshore GPS boat and buoy measurements were carried out, thus scanning the sea surface with high resolution and accuracy. Some of the marine GPS measurements were conducted along the Jason satellite subtracks for validation purposes. The Sea Surface Heights (SSH) were corrected for tidal effects by using a permanent tide gauge installation. Geoid height differences calculated from DoV and compared with GPS based SSHs showed a very good agreement. The comparison of these data sets with the gravimetric geoid model HGFFT98 revealed significant disagreements. Apart from the gravimetric geoid model, a recent altimetric one based on SSHs from the Exact Repeat Missions (ERM) of ERS1, ERS2 and TOPEX/Poseidon has been employed for validation purposes (Tziavos et al. 2005). The comparison with the altimetric geoid model resulted in smaller differences, while it was also found that the altimetric, DoV and GPS models follow the same variations in the geoid height signal. Detailed validation tests of all existing data sources are presented and discussed in this paper.

2 Available data sets

2.1 Gravimetric model

The development of the gravimetric geoid solution HGFFT98 was based on an optimal combination of free-air gravity anomalies and GPS/Leveling geoid heights available for the Hellenic area. The marine gravity data were taken from the digitisation of Morelli's maps (Behrend et al 1996), so only few gravity observations were available for the area under study. The combined solution was determined using the Multiple Input – Multiple Output System Theory (MIMOST) presented by Andritsanos (2000), Andritsanos et. al. (2001). Due to the lack of specific information about the errors in both the gravimetric and GPS/Leveling input data, simulated

noises were used as input error. Randomly distributed fields were generated using a standard deviation of ±5 mGal for the gravimetric data and ±5 cm for the GPS/Leveling ones. In the case of repeat altimetric missions an estimation of the input error Power Spectral Density PSD function can be directly evaluated using this successive information. The final solutions and the error PSD function of the MIMOST method were calculated according to the following equations:

$$\hat{N}_o = \left[H_{\hat{N}N^{gr}} \quad H_{\hat{N}N^{GPS}} \right] \left(\begin{bmatrix} P_{N_o^{gr}N_o^{gr}} & P_{N_o^{gr}N_o^{GPS}} \\ P_{N_{oa}N_o^{gr}} & P_{N_o^{GPS}N_o^{GPS}} \end{bmatrix} - \begin{bmatrix} P_{m^{gr}m^{gr}} & 0 \\ 0 & P_{m^{GPS}m^{GPS}} \end{bmatrix} \right) \begin{bmatrix} P_{N_o^{gr}N_o^{gr}} & P_{N_o^{gr}N_o^{GPS}} \\ P_{N_{oa}N_o^{gr}} & P_{N_o^{GPS}N_o^{GPS}} \end{bmatrix}^{-1} \begin{bmatrix} N_o^{gr} \\ N_o^{GPS} \end{bmatrix}$$

(eq.1)

$$P_{\hat{e}\hat{e}} = \left\{ \left[H_{\hat{N}N^{gr}} \quad H_{\hat{N}N^{GPS}} \right] \left(\begin{bmatrix} P_{N_o^{gr}N_o^{gr}} & P_{N_o^{gr}N_o^{GPS}} \\ P_{N_{oa}N_o^{gr}} & P_{N_o^{GPS}N_o^{GPS}} \end{bmatrix} - \begin{bmatrix} P_{m^{gr}m^{gr}} & 0 \\ 0 & P_{m^{GPS}m^{GPS}} \end{bmatrix} \right) - \left[\hat{H}_{\hat{N}_o N_o^{gr}} \quad \hat{H}_{\hat{N}_o N_o^{GPS}} \right] \begin{bmatrix} P_{N_o^{gr}N_o^{gr}} & P_{N_o^{gr}N_o^{GPS}} \\ P_{N_{oa}N_o^{gr}} & P_{N_o^{GPS}N_o^{GPS}} \end{bmatrix} \left(\begin{bmatrix} H^*_{\hat{N}N^{gr}} \\ H^*_{\hat{N}N^{GPS}} \end{bmatrix} - \begin{bmatrix} \hat{H}^*_{\hat{N}_o N_o^{gr}} \\ \hat{H}^*_{\hat{N}_o N_o^{GPS}} \end{bmatrix} \right) \left[\hat{H}_{\hat{N}_o N_o^{gr}} \quad \hat{H}_{\hat{N}_o N_o^{GPS}} \right] \begin{bmatrix} P_{m^{gr}m^{gr}} & 0 \\ 0 & P_{m^{GPS}m^{GPS}} \end{bmatrix} \begin{bmatrix} H^*_{\hat{N}N^{gr}} \\ H^*_{\hat{N}N^{GPS}} \end{bmatrix}$$

(eq.2)

where $\hat{N}_o$ is the combined geoid estimation, N^{gr} and N^{GPS} are the pure gravimetric and GPS/Leveling signals respectively, N_o^{gr} and N_o^{GPS} are the gravimetric and GPS/Leveling observations, m^{gr} and m^{GPS} are the input noises, H_{xy} is the theoretical operator that connects the pure input and output signals, $\hat{H}_{x_o y_o}$ is the optimum frequency impulse response function, $P_{\hat{e}\hat{e}}$ is the error PSD function and *e* is the noise of the output signal.

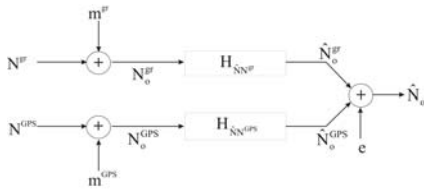

Fig. 1: A dual-input single output system for the prediction of geoid heights.

An Input-Output system of the kind described above and used for the development of the gravimetric model HGFFT98 is given in Fig. 1.

2.2 Altimetric model

The altimetric geoid model used as validation data set was computed from a combination of altimetric data from the ERM missions of ERS1/2 and TOPEX/Poseidon (T/P) (AVISO 1998). The ERS1 data (95576 point values) are taken from the 35-day ERM mission from April 14, 1992 to December 13, 1993 and March 21, 1995 to May 16, 1995 phases *c* and *g,* respectively. From ERS2, six years worth of data have been used (368617 point values) covering the period from 1995 to 2001. Finally, nine years of the T/P SSHs were employed (488634 point values) covering the period from 1992 to 2001.

The final altimetric model developed was a combination from all data sets employing least squares collocation (LSC) (Tziavos et al. 2005), by using a remove-compute-restore method. Hereby the global geopotential solution EGM96 and the effects of the bathymetry have been taken into account. In addition, the altimetric SSHs have been crossover adjusted and stacked. Thus, data over a much wider region than the area under study were used (Fig. 2).

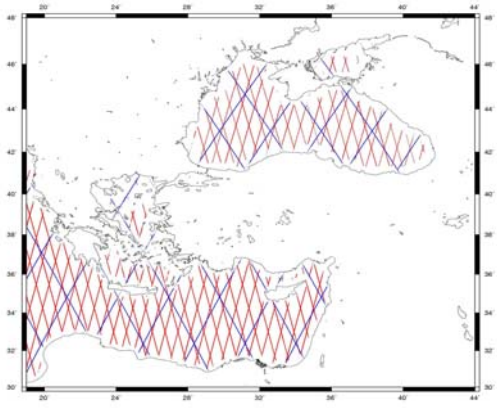

Fig. 2: Area under study for the development of the altimetric geoid and distribution of ERS1, ERS2 (gray) and T/P (black) tracks.

Moreover, the altimetric data have been reduced from the sea surface to the geoid using a local sea surface topography model developed by Rio (2004). The final altimetric geoid model for the North Aegean Sea is depicted in Fig. 3.

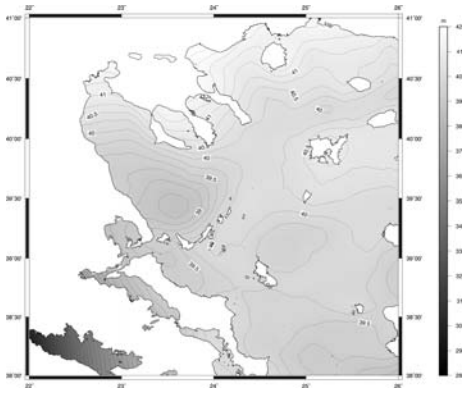

Fig. 3: The final LSC combined Mean Sea Surface model for North Aegean area.

3 Field measurements

3.1 DIADEM: Determination of Deflections of the Vertical

The digital Zenith Camera DIADEM (**Di**gital **A**stronomical **De**flection **M**easuring system) determines the physical plumb line (Φ,Λ) by directional measurements to the stars using a CCD camera (Fig. 4). The NS and WE components of the DoV (ξ,η) are determined using the following equations:

$$\xi = \Phi - \varphi \qquad \text{(eq. 3)}$$

$$\eta = (\Lambda - \lambda)\cos\varphi \qquad \text{(eq. 4)}$$

Differential GPS measurements have been carried out in order to provide geodetic coordinates with an adequate accuracy of better than 10 cm. The resulting DoV show an accuracy of about 0.15 arcsec. For detailed information about the instrumentation and method refer to Müller et al. (2004).

The distribution of Astro-stations was mainly motivated by the intention to cover the area around the North Aegean Trough (NAT), which is an important geological feature of the test area (Fig. 5). The NAT is a zone of deep water with maximum depths of up to 1500 m, trending from northeast to southwest across the North Aegean Sea. It forms the continuation of the seismically active North Anatolian Fault Zone. The NAT shows three distinctive depressions: the Sporades basin in southwest, the Mount Athos basin near Chalkidiki and the trough between the islands of Samothraki and Limnos (McNeill et al. 2004).

Fig. 4: DIADEM deployment. To determine the geodetic position the GPS antenna was put on the lens. For the astro-observations it was removed.

Fig. 5: Measuring area in the North Aegean Sea, Greece. The NAT as a zone of deep water is well recognizable.

The observations were carried out along the shoreline of the North Aegean Sea including the Sporades islands (Skiathos, Skopelos, Alonissos, Kira Panagia, Psathoura) and the islands of Thassos, Samothraki, Limnos and Agios Efstratios. Totally, 30 stations have been observed in 20 nights. In total 80 to 120 single solutions per station have been used for the determination of the direction of the local plumb line. The standard deviation of a single observation is better than 0.2 arcsec. The resulting DoV are shown in Fig. 6.

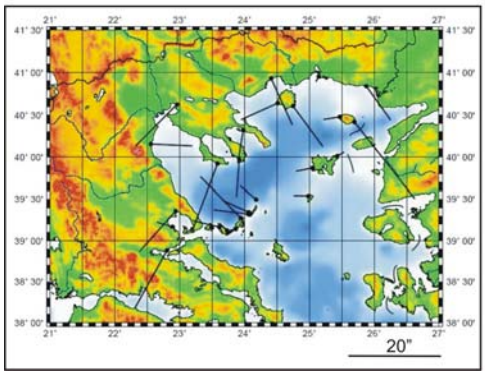

Fig. 6: DoV determined with DIADEM. The vectors shown indicate the DoV projected into the horizontal plane (components are equal to ξ and η).

The vectors on the three peninsulas of Chalkidiki, on the Sporades islands and on the islands of Thassos, Samothraki and Limnos clearly indicate the influence of the NAT representing a mass deficit with respect to the surrounding area. It is striking that on the island of Samothraki the DoV on the eastern station (Kipos) is about five times larger than on the western station (Kamariotissa) and nearly points to an opposite direction. This is mainly due to topographic and bathymetric features encountered there. The bathymetry at Kipos side shows a very steep gradient due to the trough between Limnos and Samothraki while at Kamariotissa the relief is much less inclined. The topography of the island is characterized by the Saos mountain, which reaches altitudes of up to 1600 m. This topographic mass excess causes larger gravity effects in the SE than in the NW of the island.

3.2 Marine GPS measurements: Determination of Sea Surface Heights

Enhanced ground-based methods have been developed for the precise determination of Sea Surface Heights (SSH), consisting in shipborne multi-antenna GPS measurements and GPS equipped buoys (Fig. 6). The SSH data provide local-scale information on the short-wave structure of the gravity field and can be used to improve local marine geoid solutions. They also contain information on the local dynamic ocean topography (DOT) and can be used for the validation and calibration of radar altimeter satellites. In addition, they can provide a link between offshore radar altimeter data and tide-gauge records.

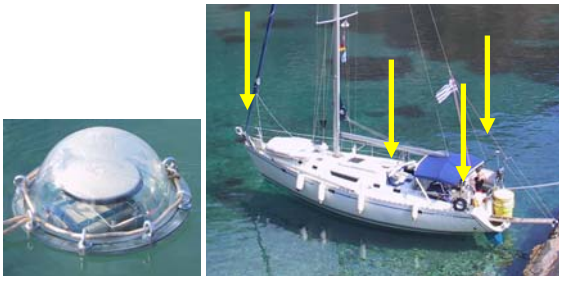

Fig. 6: Left: GPS equipped buoy (diameter 35cm) containing receiver, antenna and battery. Right: sailing boat equipped with four GPS antennas (arrows).

Highly-precise GPS positioning of the buoys and the boat is achieved by simultaneously operating the buoy receivers, the receivers aboard the boat and several permanent terrestrial GPS reference stations, all operated at a sampling rate of 1 Hz. The coordinates of the reference stations are first determined with respect to the ITRF reference frame. The kinematic positions of the buoys and the boat are then determined through differential GPS carrier phase processing with respect to the reference stations. In order to derive the Sea Surface Topography (SST) from the instantaneous SSHs, several corrections have to be applied, especially for tides and atmospheric effects (inverse barometer effect). The tide corrections have been kindly provided by E.C. Pavlis from JCET using the GOT00.2 tide model. The local tidal effects have been determined by using own tide gauges installed in the survey area. The inverse barometer corrections have been computed over the entire Mediterranean Sea using ECMWF atmospheric pressure data.

Two GPS surveys have been carried out in 2004/2005, totaling more than 1000 nautical miles of ship tracks (Fig. 7). For calibration and validation purposes of radar altimeter missions, the survey area has been chosen in the vicinity of Jason-1 ground-tracks. Dedicated buoy measurements have been performed along these Jason-1 tracks, including deployments with direct Jason-1 cross-overs, which provide precise ground-truth SSH information during the overflight.

The bathymetric low of the NAT is associated with a distinct depression of the SST, which reaches a minimum of 37.5 m above the WGS84 ellipsoid. The SST in the surrounding area is more than 39 m, reaching more than 40.5 m towards the north of the survey area (Fig. 7 and 8).

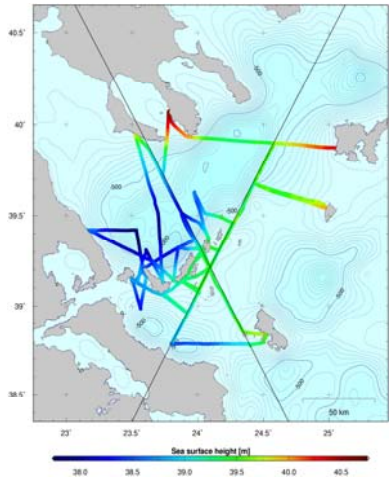

Fig. 7: Boat tracks with SSH profiles from combined shipborne/buoy GPS observations. Black lines: Jason-1 ground-tracks. Background: bathymetry.

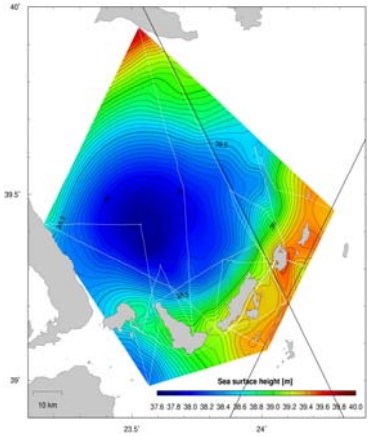

Fig. 8: Preliminary SST obtained by griding the shipborne/-buoy GPS data from the 2005 campaign (white lines). Isolines interval: 0.05 m. (Note that parts of the surface are extrapolated).

4 Results

4.1 Conversion of Deflections of the Vertical to geoid height differences

To compare DoV with SSH, they were transformed to geoid height differences ΔN using the principle of astronomical leveling. The average of the vertical deflections (ξ,η) between neighbouring stations P_i and P_{i+1} results in the component ε_i :

$$\varepsilon_i = \frac{\xi_i + \xi_{i+1}}{2} \cdot \cos\alpha_i + \frac{\eta_i + \eta_{i+1}}{2} \cdot \sin\alpha_i \qquad \text{(eq. 5)}$$

The vertical deflection ε describes the inclination of the equipotential surface in azimuth α. The equipotential profile ΔN is obtained by integrating single height increments $\varepsilon_i \cdot s_i$ from the first to the last station (n) of the profile:

$$\Delta N = -\sum_{i=1}^{n-1} \varepsilon_i \cdot s_i \qquad \text{(eq. 6)}$$

where s_i is the distance between the two stations.

4.2 Comparison of different data sets

The GPS based SSHs have been converted from the tide free to the mean tide system, and then corrected for the Mean Dynamic Sea Surface Topography (MDSST), yielding geoid heights in the mean tide system. These were re-converted to the tide free system, as the AUTH geoids are defined in this system. The overall corrections for the MDSST and the permanent tide effects were +5 cm and +1.4 cm, respectively, for the Northern Aegean Sea. By gridding the geoid heights, a preliminary shipborne geoid model (Limpach geoid) was obtained. For a comparison, the Limpach geoid as well as the gravimetric and altimetric geoids were interpolated onto profiles through selected DIADEM stations. Fig. 9 shows a representative example for a profile between Skiathos, Glossa, Skopelos, Patitiri, Gerakas, Kira Panagia South, Kira Panagia North and Psathoura. It presents the geoid height differences obtained from DoV, SSH, altimetric and gravimetric geoid. For a local comparison, all heights have been referenced to the same level based on the gravimetric solution. Concerning the relative geoid undulations, the GPS, DIADEM and altimetric data show a very good agreement. In contrast, the gravimetric geoid model reveals a significant discrepancy in the end of the profile (Patitiri-Gerakas-Kira Panagia-Psathoura) as evidenced by the relatively small slope between 60 and 80 km distance of the profile.

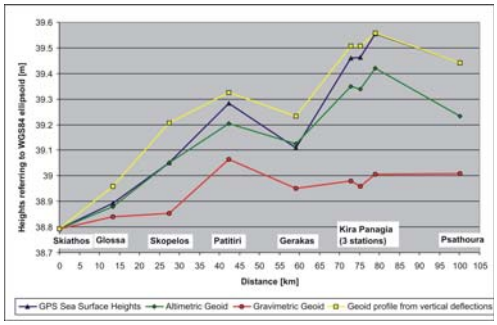

Fig. 9: Comparison between geoid height differences calculated from a) DoV b) SSH c) Altimetric geoid and d) Gravimetric geoid.

For a statistical approach, the gravimetric and the altimetric geoid models were interpolated onto the ship tracks. The heights obtained have been compared with the shipborne data. The mean difference between shipborne and gravimetric geoid heights is **70 cm** with a standard deviation of about **21 cm**.

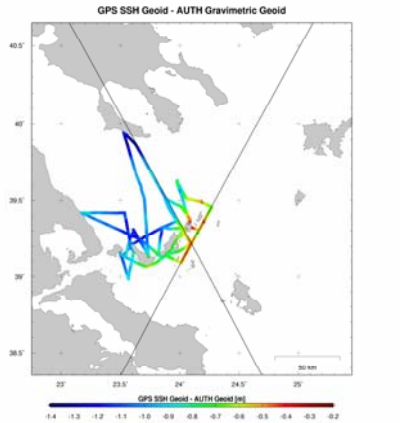

Fig. 10: Difference between Limpach geoid and gravimetric geoid model (HGFFT98) along boat tracks.

Fig. 10 illustrates the differences between the shipborne and the gravimetric geoid heights along the boat tracks. They range between –1.4 m and –0.2 m. The largest differences were found in the region of the NAT. This attributes to gravity data gaps in the marine area and the use of different reference surfaces where the available gravity data bases refer to. A comparison of shipborne and altimetric geoid heights showed a significant better agreement with a mean difference of about **4 cm** and a standard deviation of **14 cm.**

5 Conclusions

A dedicated astro-geodetic and marine GPS campaign in the North Aegean Sea has been conducted in order to validate and improve existing geoid models in this area. The marine GPS data yield instantaneous Sea Surface Heights of high spatial density that enables the determination of a Sea Surface Topography. The SST contains information on the local dynamic ocean topography and can be used to validate and calibrate satellite radar altimetric measurements. The highly-precise Deflections of the Vertical observed by the digital Zenith Camera DIADEM on several isles and at the coastline of the North Aegean Sea provide local geoid structures. They are helpful not only on islands but also in coastal areas, thus reinforcing the geoid determination in the crucial transition zone from the coast to the open sea. Geoid height differences, calculated from both data sets and compared along several profiles, showed a very good agreement within a few centimeters. The data helped to detect long wavelength errors in the gravimetric geoid model HGFFT98 from the Aristotle University of Thessaloniki. These errors are mainly due to a lack of marine gravity data in the area under study. Another reason may be the fact that the available gravity data bases refer to different reference surfaces. For the future it is planned to compute a new geoid solution by optimally combining all the available terrestrial and satellite data sources. In terms of the gravity data, a new high accuracy and resolution gravity data base for the entire Greece is under preparation.

References

Andritsanos, V.D. (2000). *Optimum combination of terrestrial and satellite data with the use of spectral methods for applications in geodesy and oceanography*. PhD Dissertation, School of Rural and Surveying Engineering, Faculty of Engineering, The Aristotle University of Thessaloniki, Department of Geodesy and Surveying.

Andritsanos, V.D., Sideris, M.G., Tziavos, I.N. (2001). *A survey of gravity field modeling applications of the Input-Output System Theory (IOST)*. IGeS Bulletin, Vol. 10, pp. 1-17.

AVISO (1998). *AVISO User Handbook – Corrected Sea Surface Heights (CORSSHs)*. AVI-NT-011-311-CN, Ed 3.1.

Behrend, D., Denker, H., Schmidt, K., (1996). *Digital gravity data sets for the mediterranean sea derived from available maps.* Bulletin d' information, No 78, pp. 31-39, BGI, 1996.

McNeill, L.C., Mille, A., Minshull, T.A., Bull, J.M., Kenyon N.H., Ivanov, M. (2004). *Extension of the North Anatolian Fault into the North Aegean Trough: Evidence for transtension, strain partitioning, and analogues for Sea of Marmara basin models.* Tectonics, Vol. 23, TC2016, 2004.

Müller, A., Bürki, B., Hirt, C., Marti, U. and Kahle, H.-G. (2004). *First Results from new High-precision Measurements of Deflections of the Vertical in Switzerland.* International Association of Geodesy Symposia, Vol. 129, Jekeli, C., Bastos, L., Fernandes, J. (eds.), Gravity Geoid and Space Missions 2004, Springer–Verlag Berlin Heidelberg, pp. 143-148.

Rio, M.-H. (2004). *A Mean Dynamic Topography of the Mediterranean Sea Estimated from the Combined use of Altimetry, In-Situ Measurements and a General Circulation Model*. Geophysical Research Letter Vol. 6, 03626.

Tziavos, I. N., Andritsanos, V. D. (1999). *Recent Geoid Computations for the Hellenic Area*. Phys. Chem. Earth (A), Vol- 24, No. 1, pp. 91-96.

Tziavos, I. N., Vergos, G. S., Kotzev V., Pashova L. (2005). *Mean sea level and sea surface topography studies in the Black Sea and the Aegean*. International Association of Geodesy Symposia, Vol. 129, Jekeli, C., Bastos, L., Fernandes, J. (eds.), Gravity Geoid and Space Missions 2004, Springer–Verlag Berlin Heidelberg, pp. 254-259.